Short communication

Peculiar substrate specificity of δ^1-pyrroline-5-carboxylate reductase in the obligately fermentative bacterium *Zymomonas mobilis*

Giuseppe Forlani [1], Boguslaw Nocek [2*], Milosz Ruszkowski [3]

✉ Giuseppe Forlani flg@unife.it 0000-0003-2598-5718

Boguslaw Nocek bnocek@anl.gov 0000-0001-8257-0792

Milosz Ruszkowski mruszkowski@ibch.poznan.pl 0000-0002-4415-3100

[1] Department of Life Science and Biotechnology, University of Ferrara, via L. Borsari 46, I-44100 Ferrara, Italy

[2] The Bioscience Division, Argonne National Laboratory, IL 60439, USA; present address: AbbVie Inc., North Chicago, Illinois, U.S.A.

[3] Institute of Bioorganic Chemistry, Polish Academy of Sciences, Noskowskiego 12/14, 61704 Poznan, Poland

[*] Present address: AbbVie Inc., North Chicago, Illinois, U.S.A.

Abstract

A *Zymomonas mobilis* gene coding for the enzyme that catalyses the last step in proline biosynthesis was cloned and heterologously expressed, and the recombinant protein was purified and characterized. Contrary to δ^1-pyrroline-5-carboxylate reductases from most other sources, it showed *in vitro* a distinct preference for NADH as the electron donor. The molecular basis of this feature was investigated by analysis of the dinucleotide binding domain *in silico*. Results are discussed in view of the obligately fermentative metabolism of this bacterium.

Keywords

electron donor • proline biosynthesis • Rossmann fold • substrate binding • substrate preference

Abbreviations

P5C, δ^1-pyrroline-5-carboxylate

Background

Besides being needed as a building block for protein synthesis, variations in the intracellular homeostasis of free proline play a role in a variety of cellular functions during development and stress adaptation [1, 2]. Moreover, the interconversion of glutamate and proline contributes to control the redox status and the NADP(H) to NAD(H) ratio in the cell [3, 4], and seems involved in the regulation of cell proliferation *vs* apoptosis [5]. As a consequence, an increasing body of evidence shows that the enzymes involved in proline metabolism are subject to a complex array of regulative mechanisms at both the transcriptional [6] and post-translational [7] levels.

δ^1-Pyrroline-5-carboxylate (P5C) reductase [EC 1.5.1.2] catalyzes the final conversion of P5C to proline in both biosynthetic pathways from glutamate and ornithine [1]. Although a few alternative routes have been described in some microorganisms [8], null mutants of P5C reductase have consequently been found embryo-lethal [9], and specific inhibitors of the enzyme exert cytotoxic effects in plants [10], bacteria [11] and human cells [12]. The enzyme has been isolated from a variety of sources but, because P5C is not commercially available, in most cases activity has been measured *in vitro* as the reverse oxidation of proline (or even proline analogue) at a non-physiological, basic pH. As a consequence, a reliable functional characterization has been performed only for a limited number of enzymes, and some features are still a matter of debate. Among them, the preference for NADPH or NADH as the co-substrate. All P5C reductases so far described can use both dinucleotides *in vitro* [13], but the effective use *in vivo* has been found questionable by the occurrence of differential inhibition by NAD^+, $NADP^+$, proline and salt, depending on whether NADH or NADPH act as the electron donor [7, 14, 15].

We previously purified and characterized P5C reductase from several sources, ranging from the bacteria *Streptococcus pyogenes* [14] and *Bacillus subtilis* [16], to the higher plants

Arabidopsis thaliana [7], *Oryza sativa* [15] and *Medicago truncatula* [17]. When the reaction of the enzyme was measured as the P5C-dependent oxidation of NAD(P)H, in all cases a clear-cut preference for NADPH as the electron donor was found. A thorough sequence analysis on the dinucleotide binding domain allowed to hypothesize about the amino acid residues involved in substrate preference [13]. However, no information was available at that time on P5C reductases with a distinct preference for NADH, though the human isoform 1 had been found able to use either electron donor with similar efficiency [18].

Here we report the characterization of P5C reductase from the facultatively anaerobic, obligately fermentative bacterium *Zymomonas mobilis*. In this case, the comparison of catalytic efficiency and product inhibition with NADH and NADPH accounted for a preferential use of the former, a result that allowed us to re-investigate the molecular basis for co-factor preference.

Methods

The sequence coding for a putative P5C reductase from *Zymomonas mobilis* (NCBI Reference Sequence: WP_011240243.1) was cloned into vector pMCSG68 that was used to overexpress the gene in *E. coli* BL21(DE3) pLysS cells. Transformation, induction by IPTG treatment and affinity purification of the enzyme were as described previously [16], with minor modifications. Protein concentration was determined by the Coomassie blue method [19], using bovine serum albumin as the standard.

P5C reductase activity was measured by following at 340 nm the P5C-dependent oxidation of NAD(P)H at 30°C. Unless otherwise specified, the reaction mixture contained, in a final volume of 200 µL, 4 mM DL-P5C and 0.5 mM NAD(P)H in 50 mM Tris-HCl buffer, pH 7.5. P5C was synthesized by the periodate oxidation of δ-*allo*-hydroxylysine. Each sample

was carried out at least in triplicate (technical replications). Every experiment was repeated twice on two different enzyme preparations (biological replications). Data were analysed using Prism 6 for Windows, version 6.03 (GraphPad Software, San Diego, CA).

In silico structural analysis was performed in UCSF Chimera [20] and Coot [21].

Results and discussion

Using homogeneous protein obtained through heterologous expression in *E. coli* and affinity purification, the functional features of *Z. mobilis* P5C reductase (*Zm*P5CR) were determined thoroughly. Results are presented in Table 1. Maximal activity ranged from 200 to 900 nkat mg^{-1} protein depending on the electron donor used, values that correspond to 6-27 catalytic events for second. The same results were obtained after removing the His_6-tail. Data reflect an unusually low catalytic rate if compared with the values obtained not only for the plant enzyme (350-4700; [7, 15, 17]), but also for other bacterial P5C reductases (20-800; [14, 16]). When the pH-activity relationship was assessed, a second, pronounced optimum was found at pH 6.5 besides the expected one at neutral pH. Concerning the electron donor, similarly to the enzyme from most other sources, higher maximal activity was evident with NADH. However, in the other cases this was counteracted by a strikingly higher affinity for NADPH, resulting in a higher or similar K_{cat}/K_M ratio. In this case, on the contrary, also a higher affinity was found for NADH (and for P5C when NADH was the co-factor as well), accounting for a 23.3-fold higher catalytic efficiency with NADH than with NADPH. If also considering that $NADP^+$ was found not inhibitory at physiological concentrations, while NAD^+ preferentially inhibited the NADPH-dependent activity (Table 1), the whole set of data suggest that in this species NADH is the preferred electron donor *in vivo*.

To investigate the molecular basis of NADH preference, amino acid sequences of all P5C reductases characterized to date by measuring the physiological reduction of P5C were

aligned (Fig. 1B). Previously, we have thoroughly investigated the coenzyme preference from a structural perspective on the basis of *M. truncatula* P5C reductase complexes with NAD^+ (PDB ID: 5bsf [17]) and $NADP^+$ (PDB ID: 5bsg). Results indicated a specific fragment in the protein sequence, a loop that interacts with the 2'O-phosphate of $NADP^+$ (motif A, Fig. 1). Three residues of the motif A (45HSN47) were directly involved in hydrogen bonding with the phosphate group. It is therefore very interesting to note a deletion of one residue in the motif A in *Z. mobilis* and in *B. cereus*, which is the next example of a bacterial species with the preference towards NADH over NADPH, with respective catalytic efficiencies ratio of 4.00 (Fig. 1). In the absence of direct structural data, we can speculate that a shorter loop of the motif A in these two species is unable to accommodate the 2'O-phosphate. Moreover, the hydrophobic side chains of Ile36 and Pro38 in *Zm*P5CR cannot H-bond the phosphate. The side chain of Arg37, although positively charged, may be too bulky and collide with the phosphate. Significance of the motif A sequence in coenzyme preference is also evident in *H. sapiens* P5C reductase isoform 1 (ratio of catalytic efficiency with NADH or NADPH of 2.88, Figure 1A). In this case, the presence of a negatively-charged Asp36 is seems responsible for electrostatic repulsion of the 2'O-phosphate (Figure 1C), even though the enzyme can bind NADPH, as shown in the crystal structure (PDB IS:5uat [22]). In summary, kinetic data on *Zm*P5CR paired with analysis of sequence variability allow to postulate the rationale for NADH specificity while supporting the motif A sequence as the main determinant of coenzyme preference in P5C reductases. It is also interesting that sequences of P5C reductases that at first appear closely related, in fact have discrete NAD(P)H preference (e.g. *B. subtilis* and *Z. mobilis*, Figure 1A). This suggests that local variations, such as in motif A, but not overall sequence identity must be considered while trying to assign a coenzyme to a particular P5C reductase *a priori*.

Z. mobilis lacks an oxidative electron transport chain and is obligately fermentative.

During glucose conversion into ethanol via the Entner-Doudoroff pathway, an early reduction of fermentative activity was reported that was accompanied by variations in nucleotide availability and a decrease of internal pH from 6.4 to 5.0 [23]. The occurrence of a pH optimum around 6.5 for P5C reductase activity seems therefore functional to maintain proline synthesis in a phase in which cell proliferation is still ongoing. Concerning nicotinamide dinucleotides, $NADP^+$ was found at a constant, very low level throughout, which seems consistent with its inability to modulate enzyme activity. On the contrary NAD^+ rapidly dropped from 4 to 1 nmol mg^{-1} protein [23], possibly relieving product inhibition and allowing in the late exponential phase of growth the use of the -more abundant- NADPH for P5C reduction. However, more experimental evidences will be needed to support these hypotheses, also taking into account that a second gene coding for a putative P5C reductase has been reported (GenBank: AAV89927.1) in this species.

Acknowledgments

This work is supported in part by the University of Ferrara within the frame of the project *FAR2019* and by the Polish National Science Centre (NCN Grant No. SONATA 2018/31/D/NZ1/03630).

Author contributions

G.F. performed biochemical characterization and drafted the paper. B.N. cloned the gene into the expression vector. M.R. performed *in silico* analysis. All authors contributed to the manuscript. All authors read and approved the final manuscript.

Compliance with ethical standards

Conflict of interest The authors declare that they have no conflict of interest.

Ethical approval This study did not require ethical approval.

Informed consent All author have seen the manuscript and approved its submission. All authors agreed with the content and all gave explicit consent to submit and they obtained consent from the responsible authorities at the institute/organization where the work has been carried out.

Data and material They are available upon request.

References

1. Trovato M, Forlani G, Signorelli S, Funck D (2019) Proline metabolism and its functions in development and stress tolerance, in: MA Hossain, V Kumar, DJ Burritt, et al. (Eds), Osmoprotectant-mediated abiotic stress tolerance in plants: recent advances and future perspectives, Springer Nature, Cham, Switzerland, 2019, pp 41–72.
2. Forlani G, Trovato M, Funck D, Signorelli S (2019) Regulation of proline accumulation and its molecular and physiological functions in stress defense, in: MA Hossain, V Kumar, DJ Burritt, et al. (Eds), Osmoprotectant-mediated abiotic stress tolerance in plants: recent advances and future perspectives, Springer Nature, Cham, Switzerland, 2019, pp 73–97.
3. Krishnan N, Dickman MB, Becker DF (2008) Proline modulates the intracellular redox environment and protects mammalian cells against oxidative stress. Free Radic Biol Med 44:671-681. https://doi.org/10.1016/j.freeradbiomed.2007.10.054
4. Shinde S, Villamor JG, Lin W, Sharma S, Verslues PE (2016) Proline coordination with fatty acid synthesis and redox metabolism of chloroplast and mitochondria. Plant Physiol 172:1074-1088. https://doi.org/10.1104/pp.16.01097

5. Guo L, Cui C, Zhang K, et al. (2019) Kindlin-2 links mechano-environment to proline synthesis and tumor growth. Nat Commun 10:845. Published 2019 Feb 19. https://doi.org/10.1038/s41467-019-08772-3
6. Zarattini M, Forlani G. (2017) Toward unveiling the mechanisms for transcriptional regulation of proline biosynthesis in the plant cell response to biotic and abiotic stress conditions. Front Plant Sci 8:927. https://doi.org/10.3389/fpls.2017.00927
7. Giberti S, Funck D, Forlani G. (2014) Δ^1-Pyrroline-5-carboxylate reductase from *Arabidopsis thaliana*: stimulation or inhibition by chloride ions and feedback regulation by proline depend on whether NADPH or NADH acts as co-substrate. New Phytol 202:911-919. https://doi.org/10.1111/nph.12701
8. Fichman Y, Gerdes SY, Kovács H, Szabados L, Zilberstein A, Csonka LN (2015) Evolution of proline biosynthesis: enzymology, bioinformatics, genetics, and transcriptional regulation. Biol Rev Camb Philos Soc 90:1065-1099. https://doi.org/10.1111/brv.12146
9. Funck D, Winter G, Baumgarten L, Forlani G (2012) Requirement of proline synthesis during Arabidopsis reproductive development. BMC Plant Biol 12:191. https://doi.org/10.1186/1471-2229-12-191
10. Forlani G, Giberti S, Berlicki L, Petrollino D, Kafarski P (2007) Plant P5C reductase as a new target for aminomethylenebisphosphonates. J Agric Food Chem 55:4340-4347. https://doi.org/10.1021/jf0701032
11. Forlani G, Petrollino D, Fusetti M, et al. (2012) Δ^1-pyrroline-5-carboxylate reductase as a new target for therapeutics: inhibition of the enzyme from *Streptococcus pyogenes* and effects in vivo. Amino Acids 42:2283-2291. https://doi.org/10.1007/s00726-011-0970-7
12. Milne K, Sun J, Zaal EA, et al. (2019) A fragment-like approach to PYCR1 inhibition. Bioorg Med Chem Lett 29:2626-2631. https://doi.org/10.1016/j.bmcl.2019.07.047
13. Forlani G, Makarova KS, Ruszkowski M, Bertazzini M, Nocek B (2015) Evolution of plant δ^1-pyrroline-5-carboxylate reductases from phylogenetic and structural perspectives. Front Plant Sci 6:567. https://doi.org/10.3389/fpls.2015.00567
14. Petrollino D, Forlani G (2012) Coenzyme preference of *Streptococcus pyogenes* δ^1-pyrroline-

5-carboxylate reductase: evidence supporting NADPH as the physiological electron donor. Amino Acids 43:493-497. https://doi.org/10.1007/s00726-011-1077-x

15. Forlani G, Bertazzini M, Zarattini M, Funck D, Ruszkowski M, Nocek B (2015) Functional properties and structural characterization of rice δ^1-pyrroline-5-carboxylate reductase. Front Plant Sci 6:565. https://doi.org/10.3389/fpls.2015.00565
16. Forlani G, Nocek B, Chakravarthy S, Joachimiak A (2017) Functional characterization of four putative δ^1-pyrroline-5-carboxylate reductases from *Bacillus subtilis*. Front Microbiol. 8:1442. https://doi.org/10.3389/fmicb.2017.01442
17. Ruszkowski M, Nocek B, Forlani G, Dauter Z (2015) The structure of *Medicago truncatula* δ^1-pyrroline-5-carboxylate reductase provides new insights into regulation of proline biosynthesis in plants. Front Plant Sci 6:869. https://doi.org/10.3389/fpls.2015.00869
18. Merrill MJ, Yeh GC, Phang JM (1989) Purified human erythrocyte pyrroline-5-carboxylate reductase. Preferential oxidation of NADPH. J Biol Chem 264:9352-9358.
19. Bradford MM (1976) A rapid and sensitive method for the quantitation of microgram quantities of protein utilizing the principle of protein-dye binding. Anal Biochem 72:248-254. https://doi.org/10.1006/abio.1976.9999
20. Pettersen EF, Goddard TD, Huang CC, et al. (2004) UCSF Chimera--a visualization system for exploratory research and analysis. J Comput Chem 25:1605-1612. https://doi.org/10.1002/jcc.20084
21. Emsley P, Lohkamp B, Scott WG, Cowtan K (2010) Features and development of Coot. Acta Crystallogr D Biol Crystallogr 66:486-501. https://doi.org/10.1107/S0907444910007493
22. Christensen EM, Patel SM, Korasick DA, et al. (2017) Resolving the cofactor-binding site in the proline biosynthetic enzyme human pyrroline-5-carboxylate reductase 1. J Biol Chem 292:7233-7243. https://doi.org/10.1074/jbc.M117.780288
23. Osman YA, Conway T, Bonetti SJ, Ingram LO (1987) Glycolytic flux in *Zymomonas mobilis*: enzyme and metabolite levels during batch fermentation. J Bacteriol 169:3726-3736. https://doi.org/10.1128/jb.169.8.3726-3736.1987
24. Madeira F, Park YM, Lee J, et al. (2019) The EMBL-EBI search and sequence analysis tools

APIs in 2019. Nucleic Acids Res 47:W636-W641. https://doi.org/10.1093/nar/gkz268

25. Yeh GC, Harris SC, Phang JM (1981) Pyrroline-5-carboxylate reductase in human erythrocytes. J Clin Invest 67:1042-1046. https://doi.org/10.1172/jci110115

Legend to figure

Fig. 1. Sequence analysis of P5C reductases for which experimental data for the catalytic efficiency of P5C reduction with either NADH and NADPH are available. Sequences have been aligned using Clustal Omega [24]. The corresponding cladogram and the ratio between catalytic efficiency (i.e. the K_{cat}/K_M ratio) with NADH and NADPH are shown in panel A. Alignment and conserved fingerprint motifs involved in dinucleotide binding (Motifs A, B, C forming the so-called Rossmann fold) are presented in panel B. The following sequences were used, with UniProt id, PDB id (if available) and reference for enzyme characterization indicated in parentheses*: Bacillus subtilis* ProG (Q00777 [16]); *Zymomonas mobilis* (Q5NQR9; this work); *Streptococcus pyogenes* M1 GAS (Q9A1S9; 2AHR [14]); *Bacillus subtilis* ProH (P0CI77 [16]); *Bacillus cereus* (Q81C08; 3GT0; Forlani and Nocek, unpublished data); *Homo sapiens* (P32322; 2GER [25]); *Oryza sativa* ssp *japonica* (Q8GT01 [15]). *Arabidopsis thaliana* (P54904 [7]); *Medicago truncatula* (G7KRM5; 5BSE; [17]). NAD^+ and $NADP^+$ binding modes with *H. sapiens* P5Cred isoform 1 (PDB ID: 2izz, unpublished) and *M. truncatula* P5C reductase (PDB ID: 5bsg [17]) are depicted in panels C and D, respectively. Both coenzymes are shown in ball-and-stick model. Protein chains are represented as light gray ribbons except for the residues next to 2'OH or 2'O-phosphate, for which main- and side-chain atoms are shown.

A

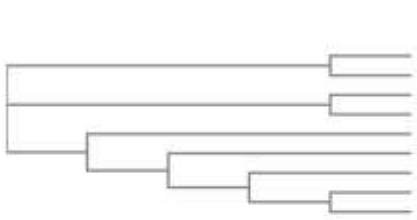

	$K_{cat}/K_{M\,(NADH)}$ / $K_{cat}/K_{M\,(NADPH)}$
B. subtilis ProG	0.068
Z. mobilis	23.3
S. pyogenes	0.124
B. subtilis ProH	0.014
B. cereus	4.00
H. sapiens is.1	2.88
O. sativa	1.14
A. thaliana	0.541
M. truncatula	0.223

B

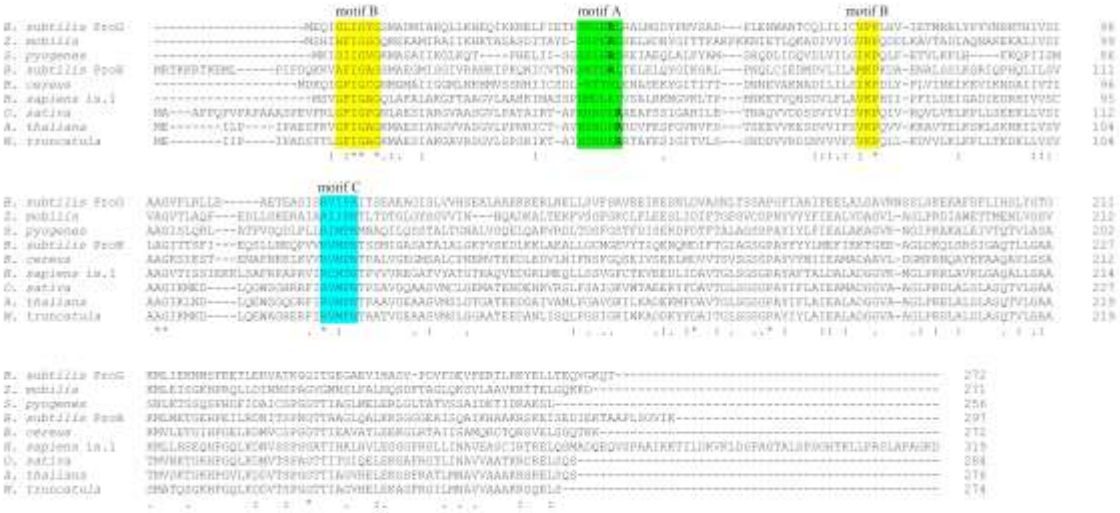

C

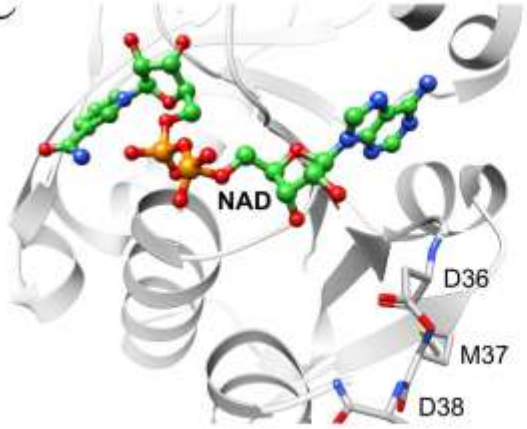

D

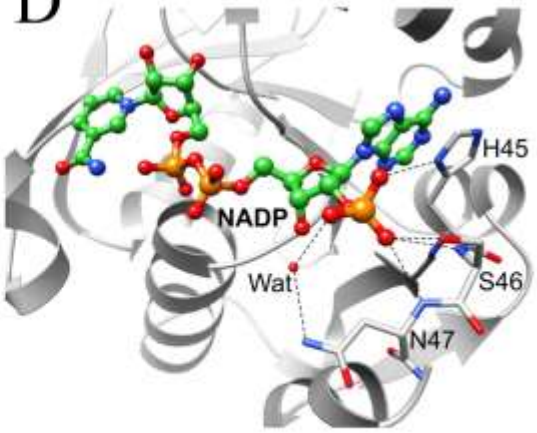

Table 1. Properties of *Zymomonas mobilis* P5C reductase.

Specific activity $_{(NADH)}$ [a]	609 ± 14 nkat (mg protein)$^{-1}$
Specific activity $_{(NADPH)}$ [a]	155 ± 4 nkat (mg protein)$^{-1}$
pH optimum [b]	6.47 ± 0.06 and 7.63 ± 0.05
$K_{M\ (app)}$ for L-P5C $_{(NADH)}$ [c]	273 ± 23 μM
$K_{M\ (app)}$ for L-P5C $_{(NADPH)}$ [c]	1053 ± 242 μM
$K_{M\ (app)}$ for NADH [c]	135 ± 9 μM
$K_{M\ (app)}$ for NADPH [c]	719 ± 91 μM
Vmax $_{(NADH)}$ [c]	892 ± 20 nkat (mg protein)$^{-1}$
Vmax $_{(P5C,\ with\ NADH\ as\ the\ co\text{-}substrate)}$ [c]	911 ± 30 nkat (mg protein)$^{-1}$
Vmax $_{(NADPH)}$ [c]	192 ± 14 nkat (mg protein)$^{-1}$
Vmax $_{(P5C,\ with\ NADPH\ as\ the\ co\text{-}substrate)}$ [c]	217 ± 36 nkat (mg protein)$^{-1}$
Kcat $_{(NADH)}$ *per* monomer [d]	27 s^{-1}
Kcat $_{(NADPH)}$ *per* monomer [d]	6 s^{-1}
$Kcat/K_{M\ (NADH)}$	1.96 • 10^5 M^{-1} s^{-1}
$Kcat/K_{M\ (NADPH)}$	0.084 • 10^5 M^{-1} s^{-1}
NAD^+ $IC_{50\ (NADH)}$ [e]	7.4 ± 0.8 mM
NAD^+ $IC_{50\ (NADPH)}$ [e]	1.4 ± 0.2 mM
$NADP^+$ $IC_{50\ (NADH)}$ [e]	22.6 ± 2.7 mM
$NADP^+$ $IC_{50\ (NADPH)}$ [e]	not inhibitory in the range tested
Proline $IC_{50\ (NADH)}$ [e]	96 ± 7 mM
Proline $IC_{50\ (NADPH)}$ [e]	107 ± 29 mM
NaCl $IC_{50\ (NADH)}$ [e]	1144 ± 105 mM
NaCl $IC_{50\ (NADPH)}$ [e]	130 ± 37 mM

[a] Specific activity was calculated under standard assay conditions at 30°C (2 mM L-P5C and 0.5 mM NAD(P)H in 50 mM Tris-HCl buffer, pH 7.5). Data are mean ± SE over three independent enzyme preparations.

[b] The pH dependence of activity was evaluated by assaying the purified enzyme for up to 5 min in the presence of 100 mM phosphate buffer, brought to the desired pH value (from 5.8 to 8.0) with KOH. The actual pH value in the reaction mixture was measured at the end of the reaction with a microelectrode. The same biphasic profile was obtained with either NADPH or NADH.

[c] Apparent affinity constants and maximal catalytic rates were estimated from the plots obtained at varying NADH or NADPH concentration at a nearly saturating P5C level, and *vice-versa*. Concentrations for the invariable substrate were 2 mM for L-P5C and 0.5 mM for NADH and NADPH. Variable substrates ranged 90-960 μM and 300-1400 μM for the couple NADPH - P5C, and 90-600 μM and 100-700 μM for the couple NADH - P5C, respectively. Data and confidence intervals were computed using the corresponding functions in Prism 6 for Windows, version 6.03 (GraphPad Software, San Diego, CA).

[d] Catalytic constant was calculated from the computed maximal catalytic rate on the basis of a molecular weight of 30.24 kDa, estimated from the cloned gene sequence and taking into account the 6-His-tail.

[e] The inhibitory effect of products and salt on enzyme activity was evaluated by measuring the P5C-dependent NAD(P)H oxidation in the presence of increasing levels of NAD^+ (0.2-25 mM), $NADP^+$ (0.1-12.5 mM), proline (10-500 mM) and NaCl (20-500 mM). Activity was expressed as percent of that in untreated controls, and the concentrations inhibiting activity by 50% (IC_{50}) and their confidence intervals were computed by using the function *log(inhibitor) vs. normalized response - variable slope* in Prism 6.